Nod1-dependent control of tumor growth

Jean da Silva Correia*, Yvonne Miranda*, Nikki Austin-Brown*, Jenny Hsu*, John Mathison*, Rong Xiang*, Huamin Zhou†, Qinxi Li†, Jiahuai Han*, and Richard J. Ulevitch*‡

*Department of Immunology, The Scripps Research Institute, 10550 North Torrey Pines Road, La Jolla, CA 92037; and †School of Life Sciences, Xiamen University, Xiamen 361005, Fujian, China

Edited by Mark T. Groudine, Fred Hutchinson Cancer Research Center, Seattle, WA, and approved December 21, 2005 (received for review October 21, 2005)

Nod1, a cytosolic protein that senses meso-diaminopimelic acid-containing ligands derived from peptidoglycan, plays a role in host responses to invasive bacteria. Here we describe a function for Nod1, whereby it controls tumor formation. Cell lines derived from the human breast cancer epithelial cell line MCF-7 were used in a severe combined immune deficiency (SCID) mouse xenograft model to characterize a pathway linking Nod1 to the growth of estrogen-sensitive tumors. In MCF-7 cells, the absence of Nod1 correlates with tumor growth, an increased sensitivity to estrogen-induced cell proliferation, and a failure to undergo Nod1-dependent apoptosis. Conversely, overexpression of Nod1 in MCF-7 cells results in inhibition of estrogen-dependent tumor growth and reduction of estrogen-induced proliferative responses *in vitro*.

apoptosis | tumor necrosis factor | MCF-7 cells | estrogen receptor

The innate immune system is composed of families of receptors that recognize components of microorganisms, viruses, or abnormal/damaged host cells. This interaction results in the initiation of host responses to eliminate and kill invading organisms or to remove atypical host cells (reviewed in refs. 1 and 2). Members of the Toll-like receptor family (TLR) have been studied extensively and linked to multiple innate immune responses. More recently, a second protein family known as the NLR/Nod/CATERPILLER/CLR family has also been linked to innate immune responses to invasive bacteria (3). The NLRs have two conserved structural features: a nucleotide-binding/oligomerization domain and leucine-rich repeat region. In contrast, the amino-terminal domain has variable structures that act as effector domains. These domains link activation of NLR/Nod family members to downstream signaling pathways and thereby determine functional responses. Nod1 (caspase recruitment domain 4; CARD4) and Nod2 (CARD15) were first described as intracellular receptors for bacterial lipopolysaccharide (LPS) (4). Now it is apparent that specific activators of Nod1 and Nod2 derive from bacterial peptidoglycan (5–8). Although minimal structural requirements for the Nod1 and Nod2 activators have been defined, formal proof of direct binding of activators is lacking.

The primary function of Nod1 and Nod2 is thought to be as sensors of invasive bacteria, and mice deficient in Nod1 or Nod2 show increased sensitivity to infection (7, 9). Because of the presence of one or two CARDs in Nod1 and Nod2, respectively, these proteins are thought to play a role in apoptosis (10). However, to date, neither has been implicated in an apoptotic pathway initiated by a specific and physiologically relevant activator. Moreover, knockout mice are viable with no obvious developmental abnormalities (11) so that programmed cell death during development does not appear to be linked to a Nod1- or Nod2-dependent function. Nonetheless, it is attractive to consider a role for Nod1- or Nod2-dependent apoptosis in a variety of biological responses. In this regard, Nod1 has been shown to associate with proteins that regulate cell death, and it appears to enhance the onset and extent of apoptosis. Moreover, transient expression of Nod1 resulted in a modest enhancement of caspase-9-induced cell death. Interestingly, overexpression of Nod1 alone is not sufficient to induce cell death (10). In humans, mutations in Nod2 are associated with an autoinflammatory disease known as Blau syndrome (12) and with increased susceptibility to Crohn's disease (13, 14). Thus there is a significant gap in our understanding of the biological settings where Nod1- or Nod2-dependent apoptosis might be important in the development of disease.

Here we have extended our knowledge about the function of the Nod1 pathway beyond its potential role in responses to infection. Specifically we provide unanticipated findings that link the Nod1 pathway to control the growth of the hormone-sensitive human breast cancer cell line, MCF-7, by using both *in vitro* cellular responses as well as data from a xenograft model of tumor growth in severe combined immune deficiency (SCID) mice. These data provide evidence that the innate immune system regulates tumor growth through hitherto unknown pathways.

Results

Nod1 Modulates Apoptosis in MCF-7 Cells. The MCF-7 breast cancer epithelial cell line is frequently used as a model to study estrogen receptor-positive breast cancer (15). We initially used this cell line to identify genes required for TNFα-induced cell death by using a retroviral-induced mutagenesis approach (16). Retroviral integration can generate null alleles resulting in diminished or abolished expression of the target gene. We determined that one of the resistant clones contained a disrupted *Nod1* gene; we termed this clone MCF-7 C20. The insertion was mapped in the *Nod1* gene between leucine-rich repeat regions 8 and 9. Western blot analysis with a monoclonal anti-human Nod1 antibody detected endogenous Nod1 protein in the parental MCF-7 cells but failed to reveal detectable expression of Nod1 in the C20 clone, suggesting that a functional allele was disrupted (Fig. 1*a*). The antibody did not detect the presence of truncated Nod1 mutants, although it was raised against the CARD of Nod1, suggesting that the *Nod*1 allele was completely repressed. We confirmed that the MCF-7 C20 clone was significantly more resistant to TNFα-induced apoptosis than the parent line (Fig. 1*b*), suggesting that Nod1 acts as a sensitizer in the TNFα pathway and links Nod1 to a ligand-dependent signaling pathway leading to apoptosis.

Thus here we used the MCF-7 cell line and various clones, including the Nod1-deficient C20 clone, derived from the parental cells, to further explore the role of Nod1 in apoptosis. We first asked whether treatment of cells with a specific Nod1 activator, Ala-γGlu-diaminopimelic acid (γTriDAP), would induce Nod1-dependent apoptosis. Light microscopic observation of MCF-7 cells treated with γTriDAP in the presence of cycloheximide (CHX) used to sensitize the cells to apoptosis (17)

Conflict of interest statement: No conflicts declared.

This paper was submitted directly (Track II) to the PNAS office.

Abbreviations: CARD, caspase recruitment domain; CHX, cycloheximide; ERα, estrogen receptor α; MDP, muramyl dipeptide; PARP, poly(ADP-ribose) polymerase; PI, propidium iodide; SCID, severe combined immune deficiency; αTriDAP, Ala-αGlu-meso-diaminopimelic acid; γTriDAP, Ala-γGlu-diaminopimelic acid.

‡To whom correspondence should be addressed. E-mail: ulevitch@scripps.edu.

www.pnas.org/cgi/doi/10.1073/pnas.0509228103

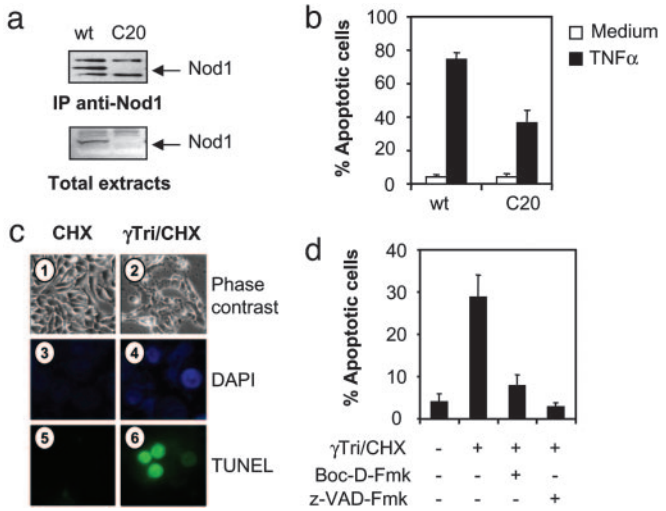

Fig. 1. Nod1 is involved in TNFα-induced apoptosis and triggers an apoptotic cascade. (*a*) Nod1 protein is absent in MCF-7 C20 cells. Cell extracts from MCF-7 parental and MCF-7 C20 cells were either immunoprecipitated with a monoclonal anti-Nod1 antibody or directly loaded on SDS/PAGE and analyzed by immunoblotting by using anti-Nod1 antibody. (*b*) MCF-7 C20 cells are more resistant to TNFα-induced apoptosis than parental cells. MCF-7 parental and MCF-7 C20 cells were treated with TNFα (10 ng/ml), and cell viability was determined by PI-exclusion assay and flow cytometry analysis. Data are expressed as mean ± SD of four independent experiments. (*c*) Morphological changes in γTriDAP-treated MCF-7 Nod1 cells. Cells were treated with γTriDAP/CHX (2, 4, 6) or CHX alone (1, 3, 5) and stained with DAPI (3, 4) or TUNEL (5, 6), fixed, and observed under a fluorescence microscope. (*d*) γTriDAP-induced apoptosis is abolished by broad-spectrum caspase inhibitors. MCF-7 Nod1 cells were pretreated with Z-VAD-Fmk or Boc-D-Fmk inhibitors (50 μM each) before addition of γTriDAP/CHX, and cell viability was measured.

revealed changes associated with apoptosis and not necrosis (Fig. 1*c*). CHX promotes apoptosis through inhibition of expression of antiapoptotic molecules such as FLIP (18). The nuclei from treated cells revealed condensed chromatin as shown by DAPI staining and also displayed nuclear fragmentation as observed by TUNEL staining. Further confirmation that γTriDAP induces apoptosis was obtained by using two broad-spectrum caspase inhibitors, z-VAD-FMK and Boc-D-FMK; both abrogated cell death (Fig. 1*d*). MCF-7 cells are known to lack caspase 3 (19), and, in studies not shown, we determined that expression of caspase 3 in parental MCF-7 cells or MCF-7 C20 cells did not change the response patterns to γTriDAP. Thus, multiple lines of evidence show that in MCF-7 cells γTriDAP induces a cell death pathway that is characteristic of apoptosis, and this effect requires the presence of Nod1 protein.

We next compared the effects of γTriDAP on the C20 clone and several additional cell lines including parental MCF-7 cells overexpressing human Nod1 (MCF-7 Nod1) and the parental line transfected with an empty retroviral vector (MCF-7 Blasto; Fig. 2). MCF-7 cells were treated with γTriDAP in the presence or absence of CHX, and cell death was determined by propidium iodide (PI) staining and flow cytometry. Exposure of wild-type cells to γTriDAP in the presence of CHX induced $\approx$25% cell death, with no death in cells treated with CHX or γTriDAP alone. The C20 cells were totally resistant to the effects of γTriDAP plus CHX, whereas the same treatment induced extensive cell death in MCF-7 Nod1 cells after 48 h of treatment. A control tripeptide, Ala-αGlu-meso-diaminopimelic acid (αTriDAP), in which meso-diaminopimelic acid is bound to Glu in the α position rather than the γ position as in γTriDAP, did not induce cell death with or without CHX. Importantly, the

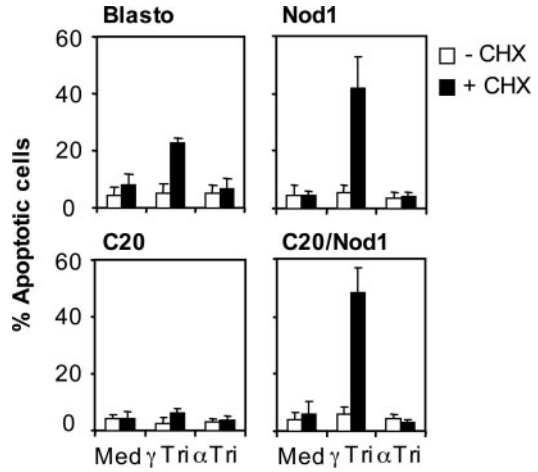

Fig. 2. Nod1 mediates γTriDAP-induced cell death. MCF-7 Blasto, MCF-7 Nod1, MCF-7 C20, and MCF-7 C20/Nod1 cells were treated with γTriDAP or αTriDAP (20 μg/ml each) in the presence or absence of CHX (3 μg/ml). Cell viability was measured by flow cytometry analysis. Data are expressed as mean ± SD of four independent experiments.

changes in sensitivity to γTriDAP shown with MCF-7 C20 cells were not seen with other proapoptotic stimuli including doxorubicin and camptothecin, where the parental and C20 clones were equally sensitive to cell death (data not shown). To show that resistance of C20 cells to γTriDAP-induced apoptosis resulted from the absence of Nod1, we stably expressed human Nod1 in MCF-7 C20 cells to produce Nod1 sufficient C20 cells (C20/Nod1). Reintroduction of Nod1 restored full sensitivity of these cells to γTriDAP-induced apoptosis (Fig. 2, lower right). In fact, we observed that overexpression of Nod1 in the C20 clone enhanced sensitivity to γTriDAP-induced apoptosis, and, likewise, stable transfectants of the parental MCF-7 line that overexpressed Nod1 also showed increase sensitivity to apoptosis when Nod1 is activated. Importantly, the ability to complement the deficient functional responses by expression of Nod1 supports our contention that the phenotype of the MCF-7 C20 cells results from a single defect, namely the failure to express Nod1.

We also examined a second breast cancer-derived cell line, SK-BR3, for the presence of a Nod1-dependent apoptotic pathway. These cells were stably transfected with Nod1, and sensitivity to γTriDAP was analyzed. Cells were treated with various combinations of TNFα and γTriDAP in the presence or absence of CHX. The percentage of apoptosis was monitored by PI staining. As shown in Fig. 3, treatment with TNFα/CHX for 24 h was slightly cytotoxic. By contrast, addition of γTriDAP dramatically enhanced apoptosis of cells exposed to TNFα/CHX (80% vs. 40%). We also characterized the activation of different members of the caspase family and monitored proteolytic processing of poly(ADP-ribose) polymerase (PARP) in SK-BR3 cells. PARP and caspases 3, 7, and 8 were cleaved completely in TNFα/CHX/γTriDAP-treated cells. Only partial processing of PARP was observed in the presence of TNFα/CHX. The presence of αTriDAP did not enhance TNFα-induced apoptosis, showing again the specificity of γTriDAP. In studies not shown here, we also determined that γTriDAP and TNFα synergize to produce cell death in MCF-7 cells, similar to what we observed with the SK-BR3 cells. In totality, these data indicate that Nod1 regulates apoptotic pathways in multiple cell lines.

Nod2 Activation Does Not Induce Apoptosis in MCF-7 Cells. Nod1 is closely related to Nod2, and, although Nod1 and Nod2 respond to different activators, few studies denote functional differences

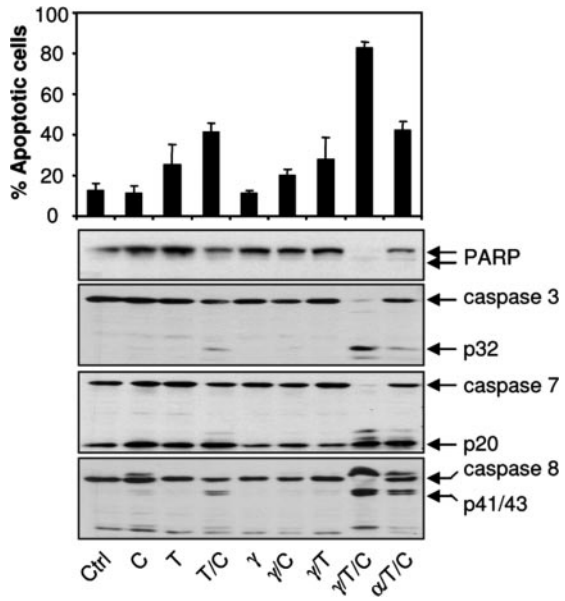

Fig. 3. Synergic activation of apoptosis by γTriDAP and TNFα in SK-BR3 cells. SKBR3 Nod1 cells were treated with various combinations of TNFα (T), γTriDAP (γ), αTriDAP (α), and CHX (C). Cells were harvested 18 h posttreatment and analyzed for cell viability by PI staining and flow cytometry (*Upper*). Data are expressed as mean ± SD of six independent experiments. Cell extracts were also prepared and subjected to immunoblotting with specific antibodies recognizing proforms and cleaved fragments of PARP and caspases 3, 7, and 8. Results show a representative experiment from three independent experiments.

between these proteins. Thus, they both activate NF-κB pathways, are believed to play a role in sensing intracellular bacteria, and are coupled to induction of a variety of cytokines. We next asked whether activation of Nod2 by its specific activator, muramyl dipeptide (MDP), would initiate apoptosis in parental MCF-7 cells or in MCF-7 cells overexpressing Nod2 (MCF-7 Nod2). In studies not shown, we used RT-PCR to determine that the parental MCF-7 cell lines expressed low amounts of mRNA encoding Nod2. We added γTriDAP or MDP in each of these lines and measured apoptosis (Fig. 4*a*) and IL-8 production (Fig. 4*b*). MCF-7 Nod2 cells treated with MDP plus CHX did not undergo apoptosis. In contrast, γTriDAP addition produced cell death as expected. MDP treatment resulted in IL-8 secretion in MCF-7 Nod2 cells. It is interesting to note that CHX was required at low doses to induce IL-8 secretion in response to γTriDAP in MCF-7 Nod1 cells and enhanced IL-8 release in response to MDP in MCF-7 Nod2 cells. Several mechanisms have been proposed to explain this effect such as increase in mRNA stability (20), increase in transcription (21), and stimulation of intracellular signaling pathways (22). Expression of Nod1 and Nod2 in MCF-7 stable transfectants was confirmed by immunoblotting (Fig. 4*c*). In studies not shown, we also determined that transfection of MCF-7 C20 cells with Nod2 did not result in apoptosis after addition of either MDP or γTriDAP. Thus it appears that there are distinct cellular pathways that determine whether activation of the Nod1 and Nod2 pathways lead to cell death and/or to up-regulation of gene activation pathways.

Nod1 Controls Tumor Formation. We next considered a number of biological processes where Nod1-dependent apoptotic pathways might be important. This evaluation included a role in regulating tumor cell growth where a failure of malignant cells to undergo cell death leads to tumorigenesis. To examine this possibility, we used a xenograft model of tumor growth in SCID mice. MCF-7 Blasto, MCF-7 C20, and MCF-7 C20/Nod1 were used to induce tumor growth in SCID/SCID or SCID/NOD mice by s.c. injection of 3×10^6 cells into the flanks of female mice. Animals were scored for tumor formation once a week after injection for up to 8 weeks. All three cell types grew similar tumors during the first weeks so that by 15 days after injection there was an approximate calculated tumor volume of 30 mm^3. Surprisingly, the tumors produced by MCF-7 Blasto and MCF-7 C20/Nod1 cells quickly diminished in size and almost disappeared. During the remaining 40 days of this experiment, the tumors formed from MCF-7 Blasto and MCF-7 C20/Nod1 cells regressed to a minimally detectable size (<10 mm^3), whereas MCF-7 C20 cells produced large round tumors, growing to a maximum volume of 200–270 mm^3, at the site of injection (Fig. 5*a Left*). Thus the absence of Nod1 allows for tumor growth. Because these studies are performed in SCID mice, the role of an immune response to the xenograft is negligible. Further, because the MCF-7 cells undergo apoptosis in response to TNFα, we performed studies

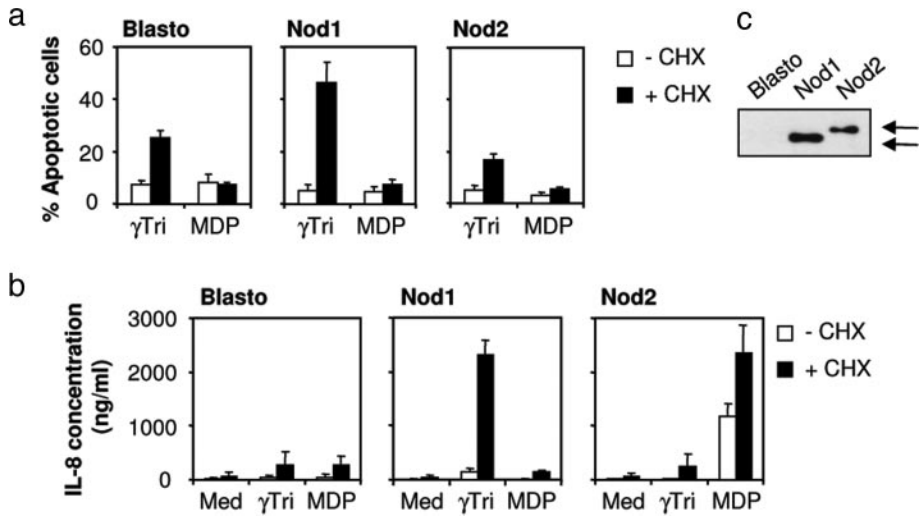

Fig. 4. Nod2 does not induce apoptosis in MCF-7 cells. MCF-7 Blasto, MCF-7 Nod1, and MCF-7 Nod2 were treated with γTriDAP or MDP (20 μg/ml each) in the presence or absence of CHX. (*a*) Cell death was measured by flow cytometry. (*b*) Cell supernatants were harvested and assayed for IL-8 secretion. Data are expressed as mean ± SD of three independent experiments. (*c*) Expression of Nod1 and Nod2 was confirmed by Western blot analysis by using anti-Myc antibody.

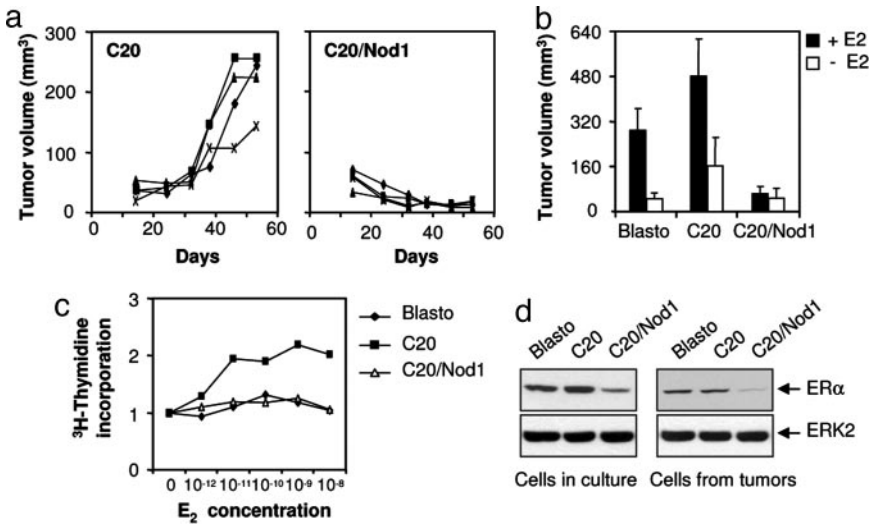

Fig. 5. The presence of Nod1 prevents tumor growth in SCID mice. (*a*) MCF-7 Blasto, MCF-7 C20, and MCF-7 C20/Nod1 cells (3×10^6 cells per mouse) were injected in the flanks of female SCID mice. Tumor size was measured once a week, and volume was determined according to the formula $(W2 \times L)/2$. Each line represents tumor growth of 1 mouse ($n = 4$). (*b*) Mice were implanted with estrogen pellets before injection with MCF-7 cells, and tumor size was determined. Mean ± SD are shown for 8 mice. (*c*) MCF-7 C20 and MCF-7 RIP2ΔCARD cells show a higher sensitivity to estrogens. Indicated MCF-7 cells were exposed to increasing concentration of 17β-estradiol and pulsed with [^{3}H]thymidine, and cell growth was determined by liquid scintillation. Data are representative of at least three independent experiments. (*d*) Down-regulation of endogenous ERα by Nod1. Total protein extracts from MCF-7 Blasto, MCF-7 C20, and MCF-7 C20/Nod1 cells and from cells isolated from tumors were analyzed by immunoblotting by using antibody against ERα and ERK2 as loading control.

by using a hamster monoclonal antibody that neutralizes murine TNFα (23). The presence of this antibody did not affect the outcome of the experiment performed exactly as described above; no tumors formed when MCF-7 Blasto or MCF-7 Nod1 cells were inoculated, whereas tumors grew when we used MCF-7 C20 cells (data not shown). The absence of tumors is not because of a decreased proliferation rate of MCF-7 Blasto and MCF-7 C20/Nod1 cells compared with MCF-7 C20. In studies not shown, we determined that each of the MCF-7 lines studied here have identical growth characteristics in tissue culture conditions and in soft agar colony-forming assays.

In most studies, tumor formation by MCF-7 cells requires supplementation of estrogens for tumorigenesis in nude mice, even when cells are inoculated at high concentration. We next decided to grow all three cell lines in mice that were implanted with estrogen pellets (Fig. 5*b*). As expected, tumors grew in mice injected with MCF-7 Blasto. Mice injected with MCF-7 C20 grew even larger tumors in the presence of estrogen pellets. Interestingly, mice that received MCF-7 C20/Nod1 did not grow tumors in the presence of estrogen pellets. These data support a critical role of Nod1 pathway in tumor growth and suggest that the presence of Nod1 acts as a brake on estrogen-dependent tumor growth. To obtain additional support for this contention, we examined the sensitivity of the MCF-7 cell lines to estrogen-induced proliferation under conditions where the cells were grown in the absence of estrogen in the culture medium. Remarkably, we found that the MCF-7 C20 cells undergo a strong proliferative response to added estrogen, whereas neither the parental or MCF-7 C20/Nod1 lines were stimulated to proliferate under identical conditions (Fig. 5*c*). The estrogen-induced proliferation observed with the MCF-7 C20 cells was blocked by addition of tamoxifen in the culture medium (data not shown). Finally, we observed that overexpression of Nod1 markedly reduced expression of endogenous estrogen receptor α (ERα) without affecting that of ERK2 used as loading control (Fig. 5*d*). Similarly, a decrease in ERα expression was also observed in recultured cells isolated from tumors. These data indicate that Nod1 pathway influences ERα expression levels and therefore the sensitivity of MCF-7 breast cancer cells to develop tumors.

Discussion

Here we describe findings that provide unanticipated information about the function of Nod1. Our results support a role for Nod1 in controlling estrogen responsiveness of MCF-7 cells, a cellular model for estrogen-sensitive breast cancer tumors. The effect of Nod1 on estrogen responsiveness was revealed in cell-based assays and, most importantly, in a xenograft model of MCF-7 dependent tumorigenesis in SCID mice. This advance in our understanding was a direct result of obtaining a Nod1-deficient clone of MCF-7 cells identified in a retrovirus-induced mutagenesis screen where genes on the TNFα-induced apoptosis pathway were being sought. We characterized a number of MCF-7 derived clones with reduced sensitivity to TNFα-induced apoptosis; one clone termed MCF-7 C20 lacks detectable Nod1 protein, and, most surprisingly, studies with the parental and C20 clone established that a Nod1-specific peptidic activator (γTriDAP) induces apoptosis. MCF-7 cells have been shown to be very sensitive to many apoptotic stimuli, and our data clearly demonstrate that recognition of a motif found in peptidoglycan by Nod1-induced cell death in physiological conditions. Most importantly, we were able to complement the retroviral induced mutation in the MCF-7 C20 clone by reintroduction of Nod1 into this clone.

The potential role of Nod1 in host responses to invasive bacteria has been identified by others (7–9). Our data now adds another function to Nod1, namely its ability to regulate the growth of estrogen-sensitive tumors formed by the MCF-7 cells in a xenograft model performed in SCID mice. Multiple lines of evidence support our contention that there is a link between Nod1 and estrogen sensitivity of MCF-7 cells. In the absence of Nod1 or when the Nod1 pathway is disabled by other means, MCF-7 cells formed large tumors in SCID mice even in the absence of estrogens. By contrast, endogenous Nod1 or overexpressed Nod1 abrogated the capacity of these cells to develop tumors. RIP2/RICK is a protein kinase that functions as a downstream mediator of Nod1 signaling (24–26). In data not shown here, we showed that the parental MCF-7 cells stably expressing the dominant negative form of RIP2 (RIP2 ΔCARD) are similar to the C20 clone insofar as being able to grow tumors in SCID mice and being highly responsive to estrogen-induced

cell proliferation, further demonstrating an important role of the Nod1 pathway in the control of tumor growth. Studies done more than two decades ago by Krueger *et al.* (27) showed that muramyl peptides containing diaminopimelic acid accumulate in the human urine, suggesting that commensal flora may provide a source of Nod1 activators. These data may warrant reexamination in view of the findings reported here to determine whether there are circulating levels of Nod1 activators present in the SCID mice.

Other factors that might control tumor growth, such as the participation of the host immune system, are ruled out by the use of SCID mice or the coadministration of neutralizing anti-murine TNFα antibody. Further, we observed that simply blocking apoptosis in the MCF-7 line by stable expression of c-FLIP/CLARP did not lead to tumor growth consistent with a key role for other Nod1-dependent events (data not shown). Thus, our data support the contention that Nod1 acts as a brake on various aspects of estrogen responsiveness in MCF-7 cells. The crosstalk between these two pathways is highlighted by the fact that Nod1 blocked estrogen-induced cell proliferation. Our studies of Nod1 in this setting open up the possibility of a more complete understanding of the molecular mechanisms involved. For example, in additional studies (J.d.S.C. and R.J.U., unpublished data), we have established a link between Nod1 and the COP9 complex (28). Others have proposed a role for one or more components of the COP9 complex in tumor growth and control of ERα degradation (29); future studies using the models we have established will allow this idea to be explored further.

In summary, these data provide insights into the physiological functions of Nod1 by linking it to pathways that control tumor cell growth. There are no reports about enhanced tumor development in mice with a deletion of the Nod1 gene. In fact there are very limited data on the Nod1 knockout mice and essentially all published work has been performed with human Nod1. The present report provides a mechanism that links innate immunity and tumor growth. Future studies will allow an assessment of the relevance of the pathway characterized here in human breast cancer and perhaps other hormone-sensitive malignancies and may lead to the development of unique therapeutic approaches to stabilize or eradicate hormone-sensitive tumors.

Materials and Methods

Retroviral Mutagenesis Screening. A clone of an MCF-7 cell, which exhibited a spontaneous survival rate of <1 in 10^6, was randomly mutated with retrovirus pDisrup. We infected 5×10^6 cells with pDisrup virus and obtained $\approx 10^4$ blasticidin-resistant clones. Blasticidin-resistant clones and control parental MCF-7 cells were treated with TNF (100 ng/ml) for 48 h. The clones were regrown and picked up 2 weeks later. Although 50 TNF resistant clones were obtained from the retrovirus mutated cells, no clone was recovered from the control parental MCF-7 cells. Total RNA was isolated from each of the clones by use of TRIzol reagent (Invitrogen). The portion of the endogenous gene that was fused with the *blasticidin+* gene was amplified by the 3′ rapid amplification of cDNA ends (RACE) technique. Reverse transcription was performed with the primer RT 5′-CCA GTG AGC AGA GTG ACG AGG ACT CGA GCT CAA GC$[T]_{17}$-3′. A nested PCR was performed with the resulting reverse transcription product with the following primers: P1/Q1 (5′-AAA GCG ATA GTG AAG GAC AGT GA-3′ and 5′-CCA GTG AGC AGA GTG ACG-3′) and P2/Q2 (5′-TGC TGC CCT CTG GTT ATG TGT GG-3′ and 5′-GAG GAC TCG AGC TCA AGC-3′). P1 and P2 are located on the *balsticidin+* gene, whereas Q1 and Q2 are on the anchor sequence of RT. The PCR products of 3′RACE and RT-PCR were directly sequenced.

Cell Culture. Human breast cancer cell lines MCF-7 and SK-BR3 were maintained in DMEM supplemented with 10% FBS, 2 mM glutamine, 100 units/ml penicillin, and 10 μg/ml streptomycin. To determine the effects of 17β-estradiol (Calbiochem), cells were cultured in phenol red-free DMEM supplemented with 5% charcoal-stripped FCS. Cells were seeded in 96-well plates with various concentration of 17β-estradiol (E_2) for 24 h and pulsed with [^{3}H]thymidine [1 μCi (1 Ci = 37 GBq) per well; MP Biomedicals, Irvine, CA]. Cells were harvested on glass fiber filters, and radioactivity was measured by liquid scintillation.

Reagents. Anti-PARP and anti-caspases 3, 7, and 9 were from Cell Signaling Technology (Beverly, MA). M2 anti-FLAG monoclonal antibody was from Sigma. Polyclonal rabbit anti-Myc antibody was from Upstate Biotechnology (Lake Placid, NY), and monoclonal anti-Myc 9E10 was from Santa Cruz Biotechnology. CHX was obtained from Sigma. Monoclonal anti-Nod1 antibody was produced in our laboratory and raised against the CARD. The broad spectrum caspase inhibitors z-VAD-FMK and Boc-D-FMK were purchased from Calbiochem. Human recombinant TNFα was purchased from R & D Systems. MDP was purchased from Bachem. γTriDAP (Ala-γGlu-meso-DAP) and αTriDAP (Ala-αGlu-meso-DAP) were chemically synthesized by AnaSpec (San Jose, CA).

Mammalian Expression Constructs and Site-Directed Mutagenesis. Human FLAG-Nod1, FLAG-Nod2, and cDNAs were obtained from G. Nuñez (University of Michigan Medical School).

Cell Viability Assays. ***PI exclusion assay.*** Cells were stimulated for indicated times. Subsequently, cells were harvested, washed twice in FACS buffer (PBS containing 1% FCS and 0.1% NaN_3), and resuspended in PI-containing FACS buffer (4 μg/ml). The extent of cell death was analyzed with a FACSCalibur flow cytometer (Becton Dickinson) by counting 10,000 cells.
DAPI staining. MCF-7 cells were plated in chamber slides and stimulated for 2 days. Apoptotic nuclei were stained with 1 μg/ml DAPI (Sigma). Cells were fixed in 4% paraformaldehyde and examined by fluorescence microscopy.
TUNEL staining. Cells were treated with γTriDAP and apoptotic nuclei were monitored by TUNEL assay according to manufacturer's instruction (Roche Applied Sciences, Indianapolis, IN).
3,3′ dihexyloxacarbocyanine iodide [DiOC6 (3)] staining. Mitochandrial membrane potential ($\Delta\Psi$m) was evaluated by staining of cells with 40 nM DiOC6 (3) (Molecular Probes) (stock solution of 1 μM in ethanol) for 20 min at 37°C. The fluorescence emitted by cells was analyzed by FACS.

Western Blot Analysis. Cells were washed extensively and lysed in lysis buffer containing 50 mM Hepes, 100 mM NaCl, 2 mM EDTA, 10% glycerol, 1% Nonidet P-40, 14 μM pepstatin A, 100 μM leupeptin, 3 mM benzamidine, 1 mM PMSF, 1 mM sodium pyrophosphate, 10 mM sodium orthovanadate, 100 units/ml aprotinin, and 100 mM sodium fluoride. Cell lysates were separated on SDS/PAGE and transferred to poly(vinylidene difluoride) membranes.

IL-8 ELISA. Concentration of IL-8 in the culture supernatants of transfected HeLa cells was measured by ELISA by using 96-well Immunlon plates (Dynatech). ELISA was performed by using the mAb MAB208 for capture and a biotinylated polyclonal rabbit anti-human IL-8 Ab (R & D Systems) followed by streptavidin horseradish peroxidase for detection.

Xenograft Model. MCF-7 Blasto, MCF-7 C20, and MCF-7 C20/Nod1 were trypsinized, washed once with PBS, and resuspended to a concentration of 1.5×10^7 cells per ml. Two hundred microliters of each suspension was inoculated s.c. in the flanks of female SCID mice. Tumor size was assessed once a week, and tumor volume was calculated.

This work was supported by National Institutes of Health Grants AI 15136 and U54 AI54523 (to R.J.U.), Novartis Grant SFP 1568 (to R.J.U.), and U.S. Army Breast Cancer Research Program Idea Award DAMD17-01-1-0389 (to J. Han).

1. Janeway, C. A., Jr., & Medzhitov, R. (2002) *Annu. Rev. Immunol.* **20,** 197–216.
2. Beutler, B. (2004) *Mol. Immunol* **40,** 845–859.
3. Ting, J. P. & Davis, B. K. (2005) *Annu. Rev. Immunol.* **23,** 387–414.
4. Inohara, N., Ogura, Y., Chen, F. F., Muto, A. & Nunez, G. (2001) *J. Biol. Chem.* **276,** 2551–2554.
5. Inohara, N., Ogura, Y., Fontalba, A., Gutierrez, O., Pons, F., Crespo, J., Fukase, K., Inamura, S., Kusumoto, S., Hashimoto, M., *et al.* (2003) *J. Biol. Chem.* **278,** 5509–5512.
6. Girardin, S. E., Boneca, I. G., Viala, J., Chamaillard, M., Labigne, A., Thomas, G., Philpott, D. J. & Sansonetti, P. J. (2003) *J. Biol. Chem.* **278,** 8869–8872.
7. Girardin, S. E., Boneca, I. G., Carneiro, L. A., Antignac, A., Jehanno, M., Viala, J., Tedin, K., Taha, M. K., Labigne, A., Zahringer, U., *et al.* (2003) *Science* **300,** 1584–1587.
8. Chamaillard, M., Hashimoto, M., Horie, Y., Masumoto, J., Qiu, S., Saab, L., Ogura, Y., Kawasaki, A., Fukase, K., Kusumoto, S., *et al.* (2003) *Nat. Immunol.* **4,** 702–707.
9. Kobayashi, K. S., Chamaillard, M., Ogura, Y., Henegariu, O., Inohara, N., Nunez, G. & Flavell, R. A. (2005) *Science* **307,** 731–734.
10. Inohara, N., Koseki, T., del Peso, L., Hu, Y., Yee, C., Chen, S., Carrio, R., Merino, J., Liu, D., Ni, J. & Nunez, G. (1999) *J. Biol. Chem.* **274,** 14560–14567.
11. Pauleau, A. L. & Murray, P. J. (2003) *Mol. Cell. Biol.* **23,** 7531–7539.
12. Miceli-Richard, C., Lesage, S., Rybojad, M., Prieur, A. M., Manouvrier-Hanu, S., Hafner, R., Chamaillard, M., Zouali, H., Thomas, G. & Hugot, J. P. (2001) *Nat. Genet.* **29,** 19–20.
13. Ogura, Y., Bonen, D. K., Inohara, N., Nicolae, D. L., Chen, F. F., Ramos, R., Britton, H., Moran, T., Karaliuskas, R., Duerr, R. H., *et al.* (2001) *Nature* **411,** 603–606.
14. Hugot, J. P., Chamaillard, M., Zouali, H., Lesage, S., Cezard, J. P., Belaiche, J., Almer, S., Tysk, C., O'Morain, C. A., Gassull, M., *et al.* (2001) *Nature* **411,** 599–603.
15. Simstein, R., Burow, M., Parker, A., Weldon, C. & Beckman, B. (2003) *Exp. Biol. Med.* **228,** 995–1003.
16. Wang, X., Ono, K., Kim, S. O., Kravchenko, V., Lin, S. C. & Han, J. (2001) *EMBO Rep.* **2,** 628–633.
17. Wu, R. C., Chen, D. F., Liu, M. J. & Wang, Z. (2004) *Biol. Pharm. Bull.* **27,** 1075–1080.
18. Santiago, B., Galindo, M., Palao, G. & Pablos, J. L. (2004) *J. Immunol.* **172,** 560–566.
19. Janicke, R. U., Sprengart, M. L., Wati, M. R. & Porter, A. G. (1998) *J. Biol. Chem.* **273,** 9357–9360.
20. Ohh, M. & Takei, F. (1995) *J. Cell Biochem.* **59,** 202–213.
21. Roger, T., Out, T. A., Jansen, H. M. & Lutter, R. (1998) *Biochim. Biophys. Acta* **1398,** 275–284.
22. Zinck, R., Cahill, M. A., Kracht, M., Sachsenmaier, C., Hipskind, R. A. & Nordheim, A. (1995) *Mol. Cell. Biol.* **15,** 4930–4938.
23. Bancroft, G. J., Sheehan, K. C., Schreiber, R. D. & Unanue, E. R. (1989) *J. Immunol.* **143,** 127–130.
24. Kobayashi, K., Inohara, N., Hernandez, L. D., Galan, J. E., Nunez, G., Janeway, C. A., Medzhitov, R. & Flavell, R. A. (2002) *Nature* **416,** 194–199.
25. Chin, A. I., Dempsey, P. W., Bruhn, K., Miller, J. F., Xu, Y. & Cheng, G. (2002) *Nature* **416,** 190–194.
26. Bertin, J., Nir, W. J., Fischer, C. M., Tayber, O. V., Errada, P. R., Grant, J. R., Keilty, J. J., Gosselin, M. L., Robison, K. E., Wong, G. H., *et al.* (1999) *J. Biol. Chem.* **274,** 12955–12958.
27. Krueger, J. M., Karnovsky, M. L., Martin, S. A., Pappenheimer, J. R., Walter, J. & Biemann, K. (1984) *J. Biol. Chem.* **259,** 12659–12662.
28. Schwechheimer, C. (2004) *Biochim. Biophys. Acta* **1695,** 45–54.
29. Callige, M., Kieffer, I. & Richard-Foy, H. (2005) *Mol. Cell. Biol.* **25,** 4349–4358.